Protein Science (2000), *9*:878–885. Cambridge University Press. Printed in the USA.

Ser45 plays an important role in managing both the equilibrium and transition state energetics of the streptavidin–biotin system

DAVID E. HYRE,[1] ISOLDE LE TRONG,[2] STEFANIE FREITAG,[2] RONALD E. STENKAMP,[2] AND PATRICK S. STAYTON[1]

[1]Department of Bioengineering, University of Washington, Seattle, Washington 98195
[2]Department of Biological Structure and the Biomolecular Structure Center, University of Washington, Seattle, Washington 98195

(RECEIVED November 23, 1999; ACCEPTED March 10, 2000)

Abstract

The contribution of the Ser45 hydrogen bond to biotin binding activation and equilibrium thermodynamics was investigated by biophysical and X-ray crystallographic studies. The S45A mutant exhibits a 1,700-fold greater dissociation rate and 907-fold lower equilibrium affinity for biotin relative to wild-type streptavidin at 37 °C, indicating a crucial role in binding energetics. The crystal structure of the biotin-bound mutant reveals only small changes from the wild-type bound structure, and the remaining hydrogen bonds to biotin retain approximately the same lengths. No additional water molecules are observed to replace the missing hydroxyl, in contrast to the previously studied D128A mutant. The equilibrium ΔG°, ΔH°, ΔS°, ΔC_P°, and activation $\Delta G^\ddagger$ of S45A at 37 °C are -13.7 ± 0.1 kcal/mol, -21.1 ± 0.5 kcal/mol, -23.7 ± 1.8 cal/mol K, -223 ± 12 cal/mol K, and 20.0 ± 2.5 kcal/mol, respectively. Eyring analysis of the large temperature dependence of the S45A off-rate resolves the $\Delta H^\ddagger$ and $\Delta S^\ddagger$ of dissociation, 25.8 ± 1.2 kcal/mol and 18.7 ± 4.3 cal/mol K. The large increases of $\Delta H^\ddagger$ and $\Delta S^\ddagger$ in the mutant, relative to wild-type, indicate that Ser45 could form a hydrogen bond with biotin in the wild-type dissociation transition state, enthalpically stabilizing it, and constraining the transition state entropically. The postulated existence of a Ser45-mediated hydrogen bond in the wild-type streptavidin transition state is consistent with potential of mean force simulations of the dissociation pathway and with molecular dynamics simulations of biotin pullout, where Ser45 is seen to form a hydrogen bond with the ureido oxygen as biotin slips past this residue after breaking the native hydrogen bonds.

Keywords: binding energetics; biotin; crystallography; hydrogen bond; streptavidin; transition state modeling

Streptavidin is a tetrameric protein known for its very high affinity binding to biotin (vitamin H; Green, 1990). In addition to its many practical uses, streptavidin serves as a useful model for studying high-affinity protein–ligand energetics. Characterizing these interactions may provide important insight for rational drug design approaches that attempt to design tight-binding molecules. Our goal is to understand the specific energetic contributions that make streptavidin–biotin such a tight-binding system.

Streptavidin employs three major motifs for strong ligand binding. First, van der Waals and hydrophobic interactions are known to play a large role, as alteration of hydrophobic side chains at the biotin binding pocket results in large losses in binding affinity (Chilkoti et al., 1995; Sano & Cantor, 1995; Dixon & Kollman, 1999). Second, a disorder-to-order transition in the binding loop at residues 45–52 that is associated with ligand binding may contribute significantly to binding energetics. Removal of this loop decreases K_a by as much as six orders of magnitude (Chu et al., 1998). Finally, a hydrogen-bonding network that extends from the biotin-binding pocket plays an important energetic role (Klumb et al., 1998; Freitag et al., 1999). Large interaction energies between these residues and an oxyanion resonance form of the ureido moiety of biotin were postulated from structural data (Weber et al., 1989, 1992). Alteration of any of the three residues that hydrogen bond to the ureido oxygen, N23, S27, or Y43, decreases binding affinity 7- to 300-fold (Klumb et al., 1998). A streptavidin with altered ligand specificity has also been constructed by altering these interactions (Reznik et al., 1998).

Reprint requests to: Patrick S. Stayton, Box 352125, Department of Bioengineering, University of Washington, Seattle, Washington 98195-2125; e-mail: stayton@u.washington.edu.

Abbreviations: ΔG°, equilibrium binding free energy (at 310 K unless stated otherwise); $\Delta H^\ddagger$, activation enthalpy for ligand dissociation; ΔS^{TS}, transition-state entropy (relative to unbound system); DSC, differential scanning calorimetry; ES-MS, electrospray mass spectrometry; ITC, isothermal titration calorimetry; PCR, polymerase chain reaction; RMSD, root-mean-square deviation; SDS-PAGE, sodium dodecyl sulfate–polyacrylamide gel electrophoresis.

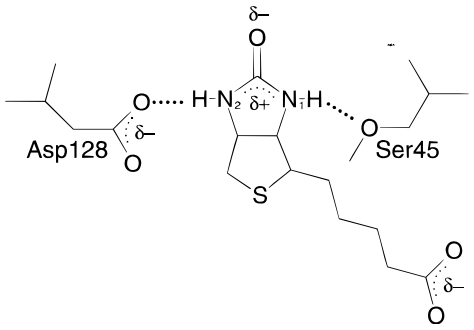

Fig. 1. Schematic of the wild-type streptavidin binding pocket (Freitag et al., 1997). Protein residues S45 and D128 are shown in relation to bound biotin. The resonance form of biotin is shown with partial charges on the ureido oxygen and nitrogens.

In addition to the strong interaction with the ureido oxygen, Weber also postulated a strong interaction between D128 and a polarized ureido nitrogen (Weber et al., 1989, 1992). A 1,000-fold decrease in binding affinity confirmed this in the D128A mutant (Freitag et al., 1999). A number of thermodynamic and structural features suggest that D128A may mimic an intermediate on the biotin dissociation pathway. We report here the structural and biophysical analysis of the Ser45Ala (S45A) mutational variant of streptavidin, which perturbs the hydrogen bonding interaction with the other ureido nitrogen. Residue S45 accepts a single hydrogen bond from the N1 ureido nitrogen of biotin, analogous to the D128/N2 interaction on the opposite face (see Fig. 1). We compare here the structural and thermodynamic alterations of the S45A mutant with the D128A mutant and find both interesting similarities and differences.

Results

Transition state thermodynamics

The S45A mutation of recombinant core streptavidin (residues 13–139) was made using mutagenic primers in a PCR protocol. The protein was expressed in BL21(DE3) *Escherichia coli* and purified by iminobiotin affinity chromatography using published protocols (Klumb et al., 1998). High purity was confirmed by SDS-PAGE, and electrospray mass spectrometry confirmed the expected mass of the mutant protein (13,255 Da). The T_m of the mutant was 78 °C, within 1 °C of the wild-type.

After initial characterization confirmed the identity, purity, and stability of the purified S45A protein, the biotin dissociation rate (k_{off}) was estimated using a cold-chase radiometric method with tritiated biotin (Klumb et al., 1998). An initial experiment run at 25 °C showed that almost all of the labeled biotin had dissociated in the first 5 min (data not shown). A fit of these data indicated a $T_{1/2}$ below 2 min, which approached the sampling period too closely to allow accurate measurement at this temperature. Therefore, the series of dissociation measurements was run at 6, 14, and 21 °C to reduce k_{off} to measurable rates. The results are shown in Figure 2. Instead of determining $\Delta H^{\ddagger}$ and $\Delta S^{\ddagger}$ from the temperature dependence of $\Delta G^{\ddagger}$ fit to individual experiments (Klumb et al., 1998), the data from all three temperatures were fit simultaneously with $\Delta H^{\ddagger}$ and $\Delta S^{\ddagger}$ in a global fitting approach, using the Eyring equation for the offrate k_{off}:

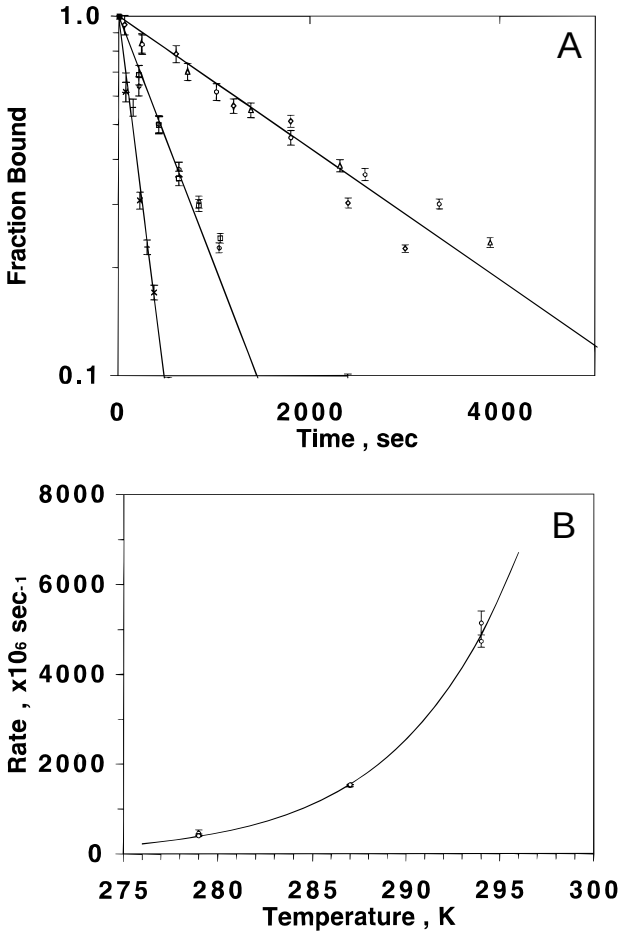

Fig. 2. Kinetics of biotin dissociation from S45A streptavidin. **A:** Global fit of all kinetic data sets at three temperatures, fit by an Eyring model with two parameters, $\Delta H^{\ddagger}$ and $\Delta S^{\ddagger}$. Each normalized data set is shown by a different symbol, with values predicted by the model fit shown as lines. **B:** Temperature dependence of the dissociation rate. Individually fit k_{off} are plotted on the line predicted by the global fit. There is a strong dependence of k_{off} on temperature, causing an 11-fold rise in off-rate between 6 and 21 °C.

$$k_{off}(T) = \frac{k_B \cdot T}{h} \cdot \exp\left(\frac{T \cdot \Delta S^{\ddagger} - \Delta H^{\ddagger}}{R \cdot T}\right) \quad (1)$$

where k_B is the Boltzmann's constant, h is Planck's constant, and R is the gas constant. The recovered values for $\Delta H^{\ddagger}$ and $\Delta S^{\ddagger}$ were 25.8 ± 1.2 kcal/mol and 18.7 ± 4.3 cal/mol K, respectively (Table 1). Based on these values, the temperature dependence of dissociation is plotted in Figure 2B with the individually fitted rates. The dissociation half-life is estimated to drop below 1 min at temperatures higher than 27 °C, while $\Delta G^{\ddagger}$ at 37 °C is calculated to be 20.0 kcal/mol.

Equilibrium thermodynamics

The equilibrium enthalpy and heat capacity changes of biotin binding (ΔH° and ΔC_P°) were measured using isothermal titration calorimetry (ITC) (Fig. 3; Table 2). Based on $K_{a,\mathrm{S45A}} \approx k_{on,\mathrm{WT}}/k_{off,\mathrm{S45A}}$, initial estimates of biotin-binding affinity in S45A put it in the tight-binding limit for ITC, $\gtrsim 10^8\ \mathrm{M}^{-1}$, where K_a cannot be

Table 1. *Activation thermodynamic parameters for streptavidin variants at 37 °C*

	k_{off} (10^{-6} s^{-1})	$T_{1/2}$ (s)	$\Delta G^{\ddagger}$ (kcal/mol)	$\Delta H^{\ddagger}$ (kcal/mol)	$T\Delta S^{\ddagger}$ (kcal/mol)	$\Delta S^{\ddagger}$ (cal/mol K)
S45A	50,000	14	20.0 ± 2.5[a]	25.8 ± 1.2	5.8 ± 1.3	18.7 ± 4.3
D128A	28,000	25	20.4 ± 2.3	20.7 ± 1.1	0.3 ± 1.2	1.0 ± 3.9
WT	29	23,697	24.6 ± 0.3	30.4 ± 0.2	5.8 ± 0.1	18.8 ± 0.3
Δ (S45A-WT)	1,700[b]	1,700[b]	−4.6 ± 2.8[c]	−4.6 ± 1.4[c]	0.0 ± 1.4[c]	0.0 ± 4.6[c]

[a]Confidence intervals at 1σ.
[b]Ratio of S45A relative to wild-type.
[c]Difference (S45A–wild-type).

determined reliably from the thermogram (total association at partial saturation (TAPS); stoichiometric binding). Therefore, the ITC experiments were performed with relatively high concentrations of protein in the cell (25–35 μM) to maximize the observed signal and ensure TAPS conditions. Subsequent data analysis indicated that TAPS was indeed achieved, and the K_a could not be determined from the data. ΔH was measured multiple times at 10, 18, 25, and 37 °C, and the resulting data were fit to obtain ΔC_P as the slope of ΔH vs. T. At 37 °C, $\Delta H^{\circ} = -21.1 \pm 0.5$ kcal/mol, and $\Delta C_P^{\circ} = -223 \pm 12$ cal/mol K.

The equilibrium affinity of S45A was determined by a competition experiment described previously (Fig. 4; Klumb et al., 1998). This method measures the absolute $\Delta\Delta G^{\circ}$ relative to wild-type streptavidin, and the equilibrium K_a can be estimated from the published value for the wild-type (Green, 1990). The experimental conditions were based on the K_a estimated from k_{off}, using this as the middle of the range explored. S45A was found to bind biotin 907 ± 87 times weaker than the wild-type at 37 °C (Table 2), within twofold of the 1,700 estimated from k_{off}. This ratio of affinities was converted to the differential $\Delta\Delta G^{\circ} = +4.2 \pm 0.1$ kcal/mol (mutant minus wild-type). Combining this with ΔH° and the values for the wild-type, $\Delta\Delta H^{\circ}$ and $\Delta\Delta S^{\circ}$ were calculated to be +7.5 ± 0.9 kcal/mol and 10.8 ± 3.1 cal/mol K at 37 °C, respectively.

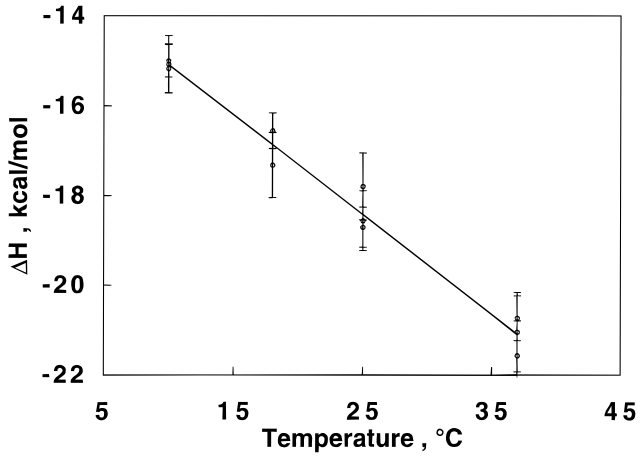

Fig. 3. Temperature dependence of equilibrium binding enthalpy measured by ITC. The slope of the fit line yields a ΔC_P° of −223 ± 12 cal/mol K.

Biotin-binding reaction coordinate

The biotin-binding reaction coordinate for S45A was derived from the equilibrium and kinetic data described above (Fig. 5). The unbound state is taken as the reference state for zero free-energy, enthalpy, and entropy change. Thus, the energies of the reference states are assumed to be equal for each variant of streptavidin. The off-rate experiments measured the barrier to dissociation from the equilibrium bound state, so the transition state placement was derived by adding the dissociation (activation) $\Delta G^{\ddagger}$, $\Delta H^{\ddagger}$, and $T\cdot\Delta S^{\ddagger}$ to the equilibrium ΔG°, ΔH°, and $T\cdot\Delta S^{\circ}$ to generate the transition-state ΔG^{TS}, ΔH^{TS}, and $T\cdot\Delta S^{TS}$, respectively. $\Delta C_P^{\ddagger}$ is assumed to be zero.

Structural characterization

An X-ray crystal structure was determined for the biotin-liganded state of S45A at 1.5 Å resolution. Crystallographic data and refinement results for the streptavidin mutant are presented in Tables 3 and 4. The streptavidin mutant described here adopts the folding found for the wild-type protein (Hendrickson et al., 1989; Weber et al., 1989). The $|F_o| - |F_c|$ difference electron density maps, with residue S45 omitted, clearly showed the mutated site.

The cocrystallization of S45A with biotin resulted in a structure with two monomers in the asymmetric unit. Monomer 1 includes residues 16–133 and monomer 2 contains residues 16–135, with the binding loops (residues 45–52) in the closed conformation. Biotin is clearly observed in the binding pocket of both monomers in the asymmetric unit. The high-resolution data made it possible to refine disordered side chains, four in each monomer. Ser27 adopts two conformations in each monomer, one of which is similar to the wild-type conformation, the other rotated 180° about χ_1. Both conformations can hydrogen bond to biotin.

Monomer 1 of the mutant biotin complex was superimposed on the wild-type biotin-bound structure using 65 Cα atoms of the core beta barrel, giving an RMSD of 0.3 Å for the superimposed atoms (Table 5; Fig. 6; Kinemage 1 (Richardson & Richardson, 1992)). Small regions of the mutant structure (biotin, the binding loop 45–52, the 23–27 loop) shift toward residue D128 by 0.2 to 0.5 Å. However, because the biotin moves along with the protein, distances from the hydrogen-binding atoms to biotin are very similar to the wild-type (Table 6). The average B-value of the biotin in S45A is 11.7 Å^2, which is similar to the biotin in the wild-type (12.9 Å^2). The mutation from serine to alanine creates a small cavity in the protein, but not one large enough to accommodate a water molecule.

Table 2. *Equilibrium thermodynamic parameters for streptavidin variants at 37 °C*

	K_d ratio factor	K_a (M^{-1})	ΔG° (kcal/mol)	ΔH° (kcal/mol)	ΔC_P° (cal/mol K)	$T\Delta S^\circ$ (kcal/mol)	ΔS° (cal/mol K)
S45A	907 ± 87[a]	4.9×10^9 ± 10%	−13.7 ± 0.1	−21.1 ± 0.5	−223 ± 12	−7.4 ± 0.6	−23.7 ± 1.8
D128A	1,032 ± 74	4.3×10^9 ± 7%	−13.7 ± 0.1	−21.5 ± 0.9	−238	−7.8 ± 0.9	−25.2 ± 2.9
WT	1	4.4×10^{12} [b]	−17.9	−28.6 ± 0.4	−345	−10.7 ± 0.4	−34.5 ± 1.3
Δ[c]	907 ± 87[d]	907 ± 10%[d]	4.2 ± 0.1[e]	7.5 ± 0.9[e]	122 ± 12[e]	3.4 ± 1[e]	10.8 ± 3.1[e]

[a]Confidence intervals at 1σ.
[b]Calculated from K_a at 25 °C = 2.5×10^{13} (Green, 1990).
[c]Ratio between S45A and wild-type.
[d]Ratio of S45A relative to wild-type.
[e]Difference (S45A–wild-type).

Discussion

The S45A streptavidin mutant was analyzed using equilibrium and kinetic methods previously applied to other mutants (Chilkoti et al., 1995; Klumb et al., 1998; Freitag et al., 1999). The location of the mutant equilibrium bound state on the ΔG° and ΔS° reaction coordinates is calculated relative to the reported ΔG° of the wild-type (Green, 1990). Any inaccuracies in this reported number will propagate into the absolute value of the mutant ΔG° and ΔS°, but the relative $\Delta\Delta G^\circ$ and $\Delta\Delta S^\circ$ will remain valid. The transition state model assumes that there is a single averaged barrier to dissociation that can be described by the Eyring transition-state theory. There are other models that could potentially be applied to the kinetic data (Hängii et al., 1990), but Eyring provides a concrete and explicit model that can be applied to analyze the temperature dependence of dissociation kinetics (unlike condensed-phase models). Were a different model to be used, the absolute value of $\Delta G^\ddagger$, $\Delta H^\ddagger$, and/or $\Delta S^\ddagger$ might be altered, but the differential ($\Delta\Delta$) values relative to the wild-type would remain largely unchanged (D.E. Hyre & P.S. Stayton, in prep.).

The energetic analysis of S45A streptavidin suggests that this residue plays an important role distinct from that played by hydrogen bonding residues previously studied (Klumb et al., 1998). S45A displays the least favorable ΔH° of all the reported hydrogen-bonding mutants and the most favorable ΔS° of the volume-conserving hydrogen-bond mutants S45A, S27A, and Y43F. N23A and Y43A have a more favorable ΔS°, but are not conservative. In the wild-type, the side chain of D128 forms a hydrogen bond with the ureido nitrogen on the opposite side of biotin, structurally mirroring the hydrogen bond of S45. The equilibrium parameters ΔG°, ΔH°, ΔS°, and ΔC_P° for S45A are most similar to those for the D128A mutant (see Table 2; Fig. 5). Weber and coworkers postulated that a ureido–oxyanion resonance form of biotin is stabilized in the bound state and increases the binding free energy through complementary electrostatic interactions (Weber et al., 1992), and the large losses of binding free energy upon mutation of ureido–oxygen hydrogen-bonding partners support this hypothesis (Klumb et al., 1998). A large interaction energy at the ureido oxygen position ($\Delta\Delta G^\circ = 3.5$ kcal) has also been calculated recently by FEP methods for mutation of the S27 side chain (Dixon & Kollman, 1999). The S45A and D128A mutants complement these claims by showing that loss of hydrogen bonds to the ureido nitrogens also significantly decreases binding free energy. These changes are similar to those observed for removal of charged hydrogen-bonding interactions (Fersht et al., 1985), suggesting the existence of polarized nitrogens and thus a polarized ureido group.

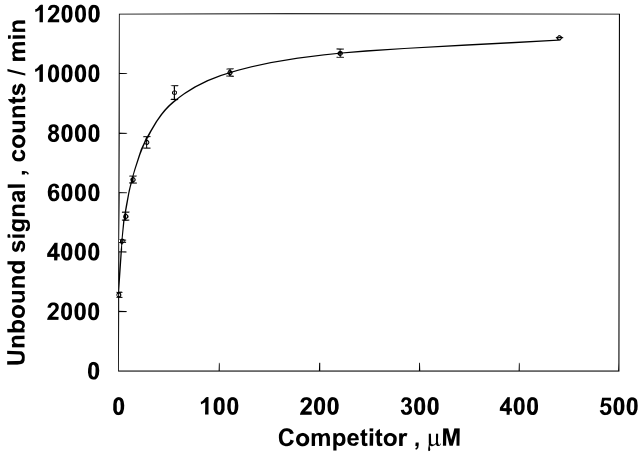

Fig. 4. Determination of $\Delta\Delta G^\circ$ for S45A relative to wild-type using a competitive radiometric method. One of six independent data sets is shown along with the line fit to the competitive binding equation described in the text (Equation 3).

The S45A and D128A mutants also appear similar to the wild-type in the transition state free energy and similar to the previously studied hydrogen bond mutants. However, the transition state and activation enthalpies and entropies (ΔH^{TS}, $\Delta H^\ddagger$, ΔS^{TS}, and $\Delta S^\ddagger$) differ significantly (Table 1). S45A displays much higher values than D128A, and higher than four of the five other hydrogen-bonding mutants studied (Klumb et al., 1998). Y43F and wild-type have larger $\Delta H^\ddagger$ and $\Delta S^\ddagger$, but lower ΔH^{TS} and ΔS^{TS}. The large $\Delta H^\ddagger$ and $\Delta S^\ddagger$ of S45A makes the biotin dissociation rate of this mutant more temperature dependent than all but Y43F and wild-type, and more rapid than all other hydrogen-bonding mutants above 17 °C. The large $\Delta H^\ddagger$ places the transition state enthalpy of S45A 2.9 kcal/mol above the wild-type and 5.5 kcal/mol above D128A. This suggests that the Ser45 hydrogen bond plays an important role in enthalpically stabilizing the transition state, because its absence leads to a large destabilization of the transition state. Similarly, the large increase in transition state entropy suggests that biotin is less constrained and has higher configurational entropy in the absence of the S45 hydrogen bond. Within the context of a single transition state model, the S45A activation

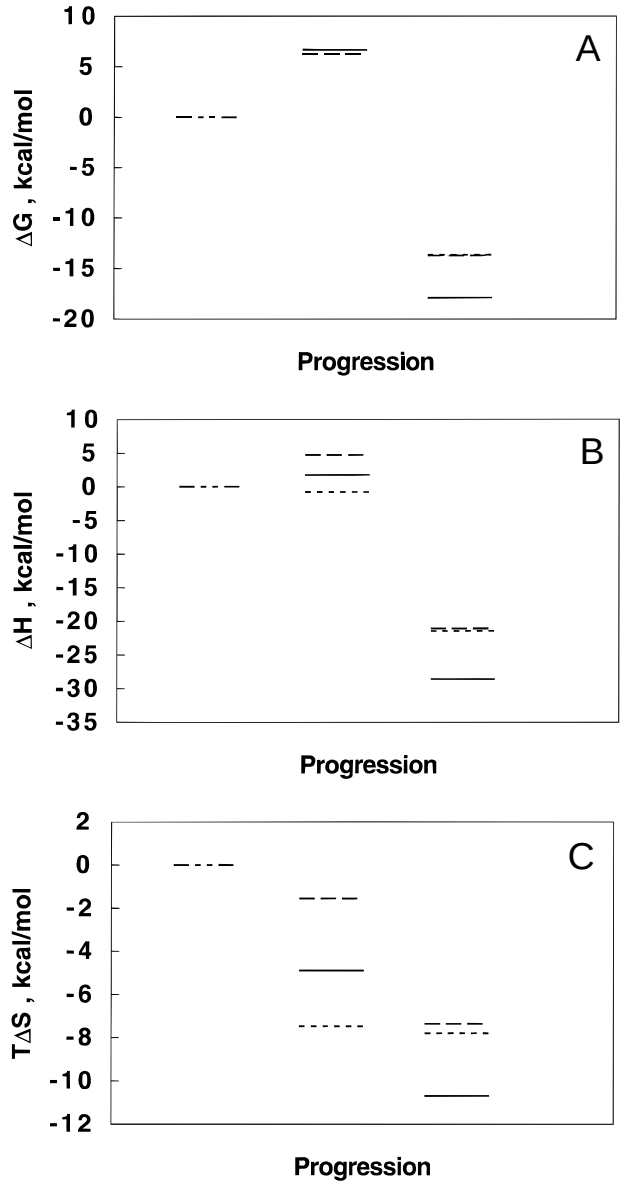

Fig. 5. Reaction coordinate diagrams for wild-type (solid line), S45A (long-dash line), and D128A (short-dash line) streptavidin. The unbound state (left) is taken as the reference state and is assumed to be equal in each mutant. The reaction coordinates were constructed from the reference state using the equilibrium binding and kinetic dissociation data. Application of a different transition state model could alter the magnitude of the vertical axis but would not alter the spacing between levels within each state.

signature is thus suggestive of the existence of an important Ser45 transitory hydrogen bond interaction in the wild-type transition state. This is consistent with observations made in the potential of mean force simulations of biotin dissociation in the wild-type, where the hydroxyl of S45 switches from accepting a hydrogen bond from the ureido nitrogen in the ground state to donating a hydrogen bond to the ureido oxygen during exit of the biotin, thus stabilizing the transition state (Freitag et al., 1999). In contrast to S45, residue D128 in the wild-type enthalpically *destabilizes* the transition state, because its absence in the D128A mutant leads to enthalpic stabilization of the transition state.

Table 3. *X-ray crystallographic data for biotin-bound S45A streptavidin*

Crystal structure parameters	
Protein	S45A-biotin
Space group	I222
Unit cell	46.2 × 94.0 × 104.6 Å
Monomers per asymmetric unit	2
Data collection and processing	
Resolution (Å)	1.5
Measured reflections	167,399
Completeness (%)	82.4
R_{merge} (%)	5.2

There are only minor structural changes in S45A relative to the wild-type. The absence of the serine hydroxyl oxygen causes the region around the mutation to shift slightly toward biotin, 0.4 Å at residue 45, only slightly larger than the differences from the wild-type observed in the core beta barrel Cα atoms (0.3 Å). In addition, the biotin shifts slightly (0.5 Å) toward the D128 carboxylate. Both these shifts are smaller in magnitude and in the opposite direction from those observed in D128A, where the shift is away from A128 and toward S45 (0.7 Å at S45 Cα, 0.8 Å in biotin ureido; Freitag et al., 1999). The hydrogen-bonding distances from biotin to the donor and acceptor atoms change little, an average of 0.1 Å (Table 6). The slight movement of biotin and binding-pocket residues away from the missing hydrogen bond and toward the remaining hydrogen bond on the other side in S45A is analogous to the shift away from the missing hydrogen bond in D128A, but much smaller in magnitude. Also, the shifts do not leave a cavity large enough for water to enter, in contrast to the water molecule that replaces the carboxylate missing in D128A.

The charge of the binding pocket is not changed by the S45A mutation, and only the one hydrogen bond from S45 to biotin is lost. Two other hydrogen bonds from the Ser45 hydroxyl to the protein backbone are lost as well, but these are second-shell changes

Table 4. *Refinement statistics for biotin-bound S45A streptavidin*

Resolution range (Å)	10–1.5
Unique reflections	30,298
All nonhydrogen atoms	2,181
Hetero atoms	32
Waters	320
R-factor $[F > 4\sigma(F)]$	0.165
R-free (10% of data)	0.217
Average *B*-values (Å^2)	
Protein	15.84
Water	31.19
Biotin	11.66
Ramachandran quality (%)	89.1
RMSD (Å)	
Bond length	0.009
Bond angles	0.029

Table 5. *RMSD values for β-barrel Cα superpositions*[a] *of streptavidin variants*

	S45A/WT	D128A/WT	S45A/D128A
Main chain	0.30–0.31[b]	0.48–0.50	0.549
Biotin	0.47–0.48	0.88–0.90	0.906
Bind-loop	0.50–0.51	0.80–0.81	0.977
23–27	0.32–0.37	1.06–1.07	1.167

[a]65 Cα residues in each of four subunits, all with biotin bound.
[b]Angstrom range observed over four monomer subunits.

Table 6. *Comparison of the average*[a] *hydrogen bond lengths (Å) in wild-type streptavidin and mutants S45A and D128A*

Biotin	Protein	WT	S45A	D128A
N1	SerOG45	3.18	NA	3.00
N2	Asp128OD2	2.86	2.73	NA
O3	Asn23ND2	2.99	2.93	3.36
O3	Ser27OG_B	2.77	2.61	2.68
O3	Tyr43OH	2.65	2.75	2.56
O2	Ser88OG	2.69	2.81	2.89
S1	Thr90OG1	3.28	3.32	3.65
RMSD from WTB			0.11	0.25

[a]Averaged over four subunits for WT and D128A, over two subunits for S45A.

that do not affect other biotin-contacting residues. A number of other mutants have also shown little change in structure relative to the wild-type, but these were not as drastically altered in binding as S45A (Freitag et al., 1998; Klumb et al., 1998). The only other mutant with comparable binding energetics is D128A, but this mutant shows significant shifts in the protein backbone, changes in the position of bound biotin, and the incorporation of an additional water molecule in the binding site (Freitag et al., 1999). We have interpreted these concerted structural alterations in D128A as mimicking an intermediate on the dissociation pathway. The number of alterations made it difficult to attribute all of the differences in binding energy directly to the loss of the D128–biotin hydrogen bond. In contrast, the relatively unchanged nature of the S45A structure suggests that a majority of the binding energy changes can be assigned to the loss of the S45–biotin hydrogen bond.

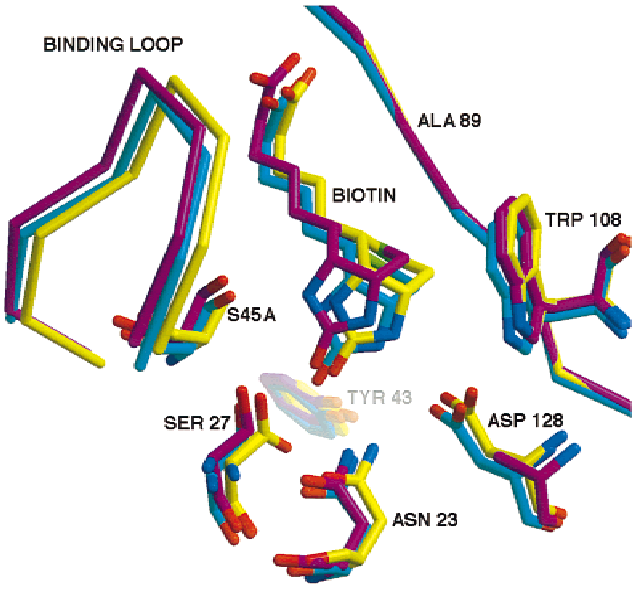

Fig. 6. Structural superposition of the bound wild-type (cyan), S45A (yellow), and D128A (magenta) streptavidin structures. The bound structures were superimposed by least-squares fit of the 65 Cα atoms in the β-barrel core of each monomer. The essentially identical structure of these cores can be seen in the overlay of the β-sheet backbone in the upper right region of the figure. The surface of the protein around S45(A) and the biotin adjust a small amount to the effects of the mutations, moving inward slightly toward D128 in the S45A mutant and outward a larger amount toward S45 in the D128A mutant.

Conclusion

The mutation of S45 to alanine results in large changes in the equilibrium affinity and dissociation rate of biotin, by three orders of magnitude in both cases. The relatively unchanged structure of mutant S45A indicates that most of the observed changes in mutant binding can be attributed to the loss of the S45-mediated hydrogen bond. The loss of the S45 hydroxyl leads to a large enthalpic destabilization of the transition state, but the effect is entirely compensated by a favorable increase in activation entropy. These signatures suggest that in addition to playing a key role in stabilizing the bound state, the Ser45 hydroxyl may also manage the activation entropy by interacting with biotin in the transition state. This transition state role is consistent with prior computational studies of the biotin dissociation pathway, where Ser45 forms a hydrogen bond with the ureido oxygen as biotin moves out of the binding pocket.

Materials and methods

Gene construction, expression, protein purification, and characterization

The S45A gene was constructed from the synthetic wild-type core streptavidin gene in pET21a (Novagen, Madison, Wisconsin) using the Stratagene QuikChange kit (Stratagene, La Jolla, California). Primers were designed to minimize secondary hybridization to sequences outside the target mutation site, to prevent hairpin formation, to have two G/C base pairs at the 3′ end of the target hybridization site, and to leave the 3′ end unpaired at alternate sites to prevent extension of the primers hybridized to these sites. The primer sequences were 5′-cagcgttaccaacagcAGCttcgtaggtaccgg-3′ and 5′-ccggtacctacgaaGCTgctgttggtaacgctg-3′. The protein was expressed from the pET21a plasmid in *E. coli*, BL21(DE3) (Novagen), refolded from guanidine-solubilized inclusion bodies by rapid dilution into buffer, and purified on an iminobiotin column as reported (Chilkoti et al., 1995). The protein showed a single band by SDS-PAGE and a single peak at the expected mass in ES-MS. The binding activity was quantified by titrating the protein with fluorescein-biotin and observing the quenching of fluorescence upon binding. It bound stoichiometrically, indicating pure and functional protein.

Kinetic measurements

The rate of biotin dissociation from S45A streptavidin was measured at 6, 14, and 21 °C by the cold-chase radiometric method published previously (Klumb et al., 1998). Briefly, 20 μM $^3H_{8,9}$-biotin was equilibrated at the experimental temperature for 1 to 2 h with 30 μM streptavidin in 2.0 mL NaCl/phosphate buffer pH 7.0. Five microliters of 15 mM unlabeled biotin was added and stirred rapidly. Three hundred microliter aliquots were removed periodically and ultrafiltered for 45 s (30 kDa MicroCon; Amicon, Inc., Beverly, Massachusetts). The filtrate was counted to determine the amount of labeled biotin released during the sampling period. Dissociation curves were normalized by measurements of labeled biotin activity and of initial counts before addition of cold biotin.

Each data set was fit by a one-term exponential decay to determine k_{off} at that temperature. These individual values of k_{off} were used as initial values in a global fit of all data, wherein the two activation parameters $\Delta H^{\ddagger}$ and $\Delta S^{\ddagger}$ were the only adjustable parameters optimized to describe all data sets using the combined, temperature-dependent exponential decay equation

$$I_t = I_0 \cdot \left\{ 1 - \exp\left[-\frac{k_B \cdot T}{h} \cdot \exp\left(\frac{T \cdot \Delta S^{\ddagger} - \Delta H^{\ddagger}}{R \cdot T} \right) \cdot t \right] \right\} \qquad (2)$$

where I_t is the observed ^{3}H count at time t, I_0 is the initial ^{3}H count, k_B is Boltzmann's constant, T is temperature (K), h is Planck's constant, and R is the gas constant. Confidence intervals of the parameters were determined by a support-plane method (Johnson & Frasier, 1985). Individual curves were checked for biphasic character, but none was found.

Equilibrium measurements: ITC, competition

Equilibrium binding enthalpies were measured at 10, 18, 25, and 37 °C on a CSC ITC-4200 isothermal titration calorimeter as reported previously (CSC, Provo, Utah), using overfill conditions. Briefly, 5 μL aliquots of 750 μM biotin were injected into 30 μM streptavidin in pH 7 phosphate–NaCl buffer. Heat flow was integrated in DataWorks (CSC) and fit in BindWorks (Applied Thermodynamics, Hunt Valley, Maryland). Standard deviation of the binding enthalpy in each experiment was derived from the standard deviation of the individual binding heats because the experiments were run under tight-binding conditions (total association at partial saturation). ΔC_P was determined as the slope of ΔH° vs. T by fitting the complete set of binding enthalpies with ΔH° and ΔC_P° terms in $\Delta H_{EXP} = \Delta H^{\circ} + \Delta C_P^{\circ} \cdot (T^{\circ} - T_{EXP})$.

Equilibrium binding affinity was determined by a radiometric competition protocol described previously (Klumb et al., 1998) with slight modifications. Increasing amounts of S45A streptavidin (60 nM to 440 μM) competed for 20 nM biotin bound to 30 nM HisTag wild-type streptavidin at 37 °C. The distribution of biotin between proteins was measured by separating out the HisTag wild-type protein through precipitation by Ni-NTA beads and counting the biotin remaining in solution. These counts were fit as the root of the described equation for binding

$$\frac{K_C}{K_P} \cdot [C \cdot L]^2 + \left(L_T + C_T + \frac{K_C}{K_P} \cdot (P_T - L_T) \right) \cdot [C \cdot L] - L_T C_T = 0 \qquad (3)$$

where K_C and K_P are the equilibrium dissociation constants for the competing (S45A) and reference (wild-type) proteins, and $[C \cdot L]$, L_T, C_T, and P_T are the concentrations of competitor-bound ligand, total ligand, total competitor protein, and total reference protein, respectively.

Crystallography

The S45A–biotin complex crystals were obtained from 40% saturated ammonium sulfate, 0.1 M sodium acetate pH 4.5 and 3.8 mM biotin and grew as blocks to a size of 0.4 × 0.3 × 0.3 mm. Biotin-bound S45A crystallized with two monomers in the asymmetric unit in an orthorhombic crystal form. The crystal form of the S45A–biotin complex has been previously described (Pahler et al., 1987; Weber et al., 1992; Hemming et al., 1995). The cell parameters and space groups of the crystals are given in Table 3.

S45A–biotin bound crystals were transferred to a cryosolution containing 42% saturated ammonium sulfate, 0.1 M sodium acetate pH 4.5, and 30% glycerol, and then mounted in a fiber loop. Data for S45A-biotin were collected on an R-axisII image plate detector system (Rigaku RU 200 rotating X-ray generator) at 125 K, processed with Denzo (Otwinowski & Minor, 1997), and scaled with SCALEPACK (Otwinowski & Minor, 1997). The crystals diffracted to 1.5 Å. Further information about the data set is summarized in Tables 3 and 4.

The molecular replacement program AMoRe (Navaza, 1994) was used to solve the structure of the S45A–biotin complex. A wild-type streptavidin model (1SWC) served as the search molecule. The binding loop (45–52) and solvent molecules were excluded for the initial refinements. The structure was refined against squares of the structure factor amplitudes (F^2) with the program SHELXL-97 (Sheldrick & Schneider, 1997). Ten percent of the data were used for the calculation of R_{free} (Brünger, 1992), but were included in the last refinement cycle. The first refinement steps were full matrix least-squares rigid body refinement for the dimer and for the separate monomers. Conjugate gradient least-squares methods were used and all parameters (coordinates and isotropic temperature factors) were refined together after the first rounds of refinement. Distance, planarity, and chiral volume restraints were applied, as were antibumping restraints. The target values for 1,2- and 1,3-distances were based on the Engh and Huber study (1991). For the isotropic temperature factors, similarity restraints were applied. Diffuse solvent regions were modeled using Babinet's principle (Moews & Kretsinger, 1975). Several second conformations of side chains were found. SHELXPRO was used for file formatting, model, and data analysis, and calculations of sigma A weighted $|F_o| - |F_c|$ and $2|F_o| - |F_c|$ coefficients (Read, 1986). The graphical evaluation of the model and electron density maps was carried out with XtalView (McRee, 1992). Most of the refined water positions were found by SHELXWAT, and the geometry of all waters was checked interactively. Water oxygen atoms were rejected when B-values increased above 63 Å^2 (U = 0.8 Å^2). The hydrogen atoms were set to idealized positions and refined with a riding model (Table 4). RMSDs for least-squares fits were calculated using Cα atoms of the β-sheet region (residues 19–23, 28–33, 38–42, 54–60, 71–80, 85–97, 103–112, 123–131). The stereochemistry was checked with the program PROCHECK (Laskowski et al., 1993) and WHATIF (Vriend & Sander, 1993). Coordinates and structure factors for this structure have been deposited in the Protein Data Bank (ID# 1DF8).

Supplementary material to the Electronic Appendix

One Kinemage file showing superposition of biotin-bound WT, S45A, and D128A streptavidin; "s45a-sa.kin."

Acknowledgments

We thank Drs. Julie Penzotti and Terry Lybrand for further discussion of the molecular dynamics simulations of wild-type streptavidin. We thank the Murdock Foundation for its support of the Biomolecular Structure Center. This research was supported by NIH Grant DK49655.

References

Brünger AT. 1992. Free *R*-value: A novel statistical quantity for assessing the accuracy of crystal structures. *Nature 355*:472–475.

Chilkoti A, Tan PH, Stayton PS. 1995. Site-directed mutagenesis studies of the high-affinity streptavidin–biotin complex: Contributions of tryptophan residues 79, 108, and 120. *Proc Natl Acad Sci USA 92*:1754–1758.

Chu V, Freitag S, Le Trong I, Stenkamp RE, Stayton PS. 1998. Thermodynamic and structural consequences of flexible loop deletion by circular permutation in the streptavidin biotin system. *Protein Sci 7*:848–859.

Dixon RW, Kollman P. 1999. The free energies for mutating S27 and W79 to alanine in streptavidin and its biotin complex: The relative size of polar and nonpolar free energies on biotin binding. *Proteins 36*:471–473.

Engh RA, Huber R. 1991. Accurate bond and angle parameters for X-ray protein structure refinement. *Acta Crystallogr A47*:392–400.

Fersht AR, Shi J-P, Jack K-J, Lowe DM, Wilkinson AJ. 1985. Hydrogen bonding and biological specificity analysed by protein engineering. *Nature 314*:235–238.

Freitag S, Chu V, Penzotti JE, Klumb LA, To R, Hyre DE, Le Trong I, Lybrand TP, Stenkamp RE, Stayton PS. 1999. A structural snapshot of an intermediate on the streptavidin–biotin dissociation pathway. *Proc Natl Acad Sci USA 96*:8384–8389.

Freitag S, Le Trong I, Chilkoti A, Klumb LA, Stayton PS, Stenkamp RE. 1998. Structural studies of binding site tryptophan mutants in the high-affinity streptavidin–biotin complex. *J Mol Biol 279*:211–221.

Freitag S, Le Trong I, Klumb LA, Stayton PS, Stenkamp RE. 1997. Structural studies of the streptavidin binding loop. *Protein Sci 6*:1157–1166.

Green NM. 1990. Avidin and streptavidin. *Methods Enzymol 184*:51–67.

Hängii P, Talkner P, Borkovec M. 1990. Reaction-rate theory: Fifty years after Kramers. *Rev Mod Phys 62*:251–342.

Hemming SA, Bochkarev A, Darst SA, Kornberg RD, Ala P, Yang DS, Edwards AM. 1995. The mechanism of protein crystal growth from lipid layers. *J Mol Biol 246*:308–316.

Hendrickson WA, Pahler A, Smith JL, Satow Y, Merritt EA, Phizackerley RP. 1989. Crystal structure of core streptavidin determined from multiwavelength anomalous diffraction of synchrotron radiation. *Proc Natl Acad Sci USA 86*:2190–2194.

Johnson ML, Frasier SG. 1985. Nonlinear least-squares analysis. *Methods Enzymol 117*:301–342.

Klumb LA, Chu V, Stayton PS. 1998. Energetic roles of hydrogen bonds at the ureido oxygen binding pocket in the streptavidin–biotin complex. *Biochemistry 37*:7657–7663.

Laskowski RA, MacArthur MW, Moss DS, Thornton JM. 1993. PROCHECK: A program to check the stereochemical quality of protein structures. *J Appl Crystallogr 26*:283–291.

McRee DE. 1992. A visual protein crystallographic software system for X11/XView. *J Mol Graph 10*:44–46.

Moews PC, Kretsinger RH. 1975. Refinement of the structure of carp muscle calcium-binding parvalbumin by model building and difference Fourier analysis. *J Mol Biol 91*:201–228.

Navaza J. 1994. AMoRe: An automated package for molecular replacement. *Acta Crystallogr A50*:157–163.

Otwinowski Z, Minor W. 1997. Processing of X-ray diffraction data collected in oscillation mode. *Methods Enzymol 276*:307–325.

Pahler A, Hendrickson WA, Kolks MA, Argarana CE, Cantor CR. 1987. Characterization and crystallization of core streptavidin. *J Biol Chem 262*:13933–13937.

Read RJ. 1986. Improved Fourier coefficients for maps using phases from partial structures with errors. *Acta Crystallogr A42*:140–149.

Reznik GO, Vajda S, Sano T, Cantor CR. 1998. A streptavidin mutant with altered ligand-binding specificity. *Proc Natl Acad Sci USA 95*:13525–13530.

Richardson DC, Richardson JS. 1992. The kinemage: A tool for scientific communication. *Protein Sci 1*:3–9.

Sano T, Cantor CR. 1995. Intersubunit contacts made by tryptophan 120 with biotin are essential for both strong biotin binding and biotin-induced tighter subunit association of streptavidin. *Proc Natl Acad Sci USA 92*:3180–3184.

Sheldrick GM, Schneider TR. 1997. SHELXL: High-resolution refinement. *Methods Enzymol 277*:319–343.

Vriend G, Sander C. 1993. Quality control of protein models: Directional atomic contact analysis. *J Appl Crystallogr 26*:47–60.

Weber PC, Ohlendorf DH, Wendoloski JJ, Salemme FR. 1989. Structural origins of high-affinity biotin binding to streptavidin. *Science 243*:85–88.

Weber PC, Wendoloski JJ, Pantoliano MW, Salemme FR. 1992. Crystallographic and thermodynamic comparison of natural and synthetic ligands bound to streptavidin. *J Am Chem Soc 114*:3197–3200.